Supporting Information for

Factors that Control Catalytic Two- vs Four-Electron Reduction of Dioxygen by Copper Complexes

Shunichi Fukuzumi,*^{,†,§} Laleh Tahsini,[†] Yong-Min Lee,[†] Kei Ohkubo,[§] Wonwoo Nam,*[,†] and Kenneth D. Karlin*[,†,‡]

[†]*Department of Bioinspired Science, Ewha Womans University, Seoul 120-750, Korea,*

[§]*Department of Material and Life Science, Graduate School of Engineering, Osaka University, Suita, Osaka 565-0871, Japan,*

[‡]*Department of Chemistry, The Johns Hopkins University, Baltimore, MD 21218, USA,*

AUTHOR EMAIL ADDRESS fukuzumi@chem.eng.osaka-u.ac.jp, karlin@jhu.edu, wwnam@ewha.ac.kr

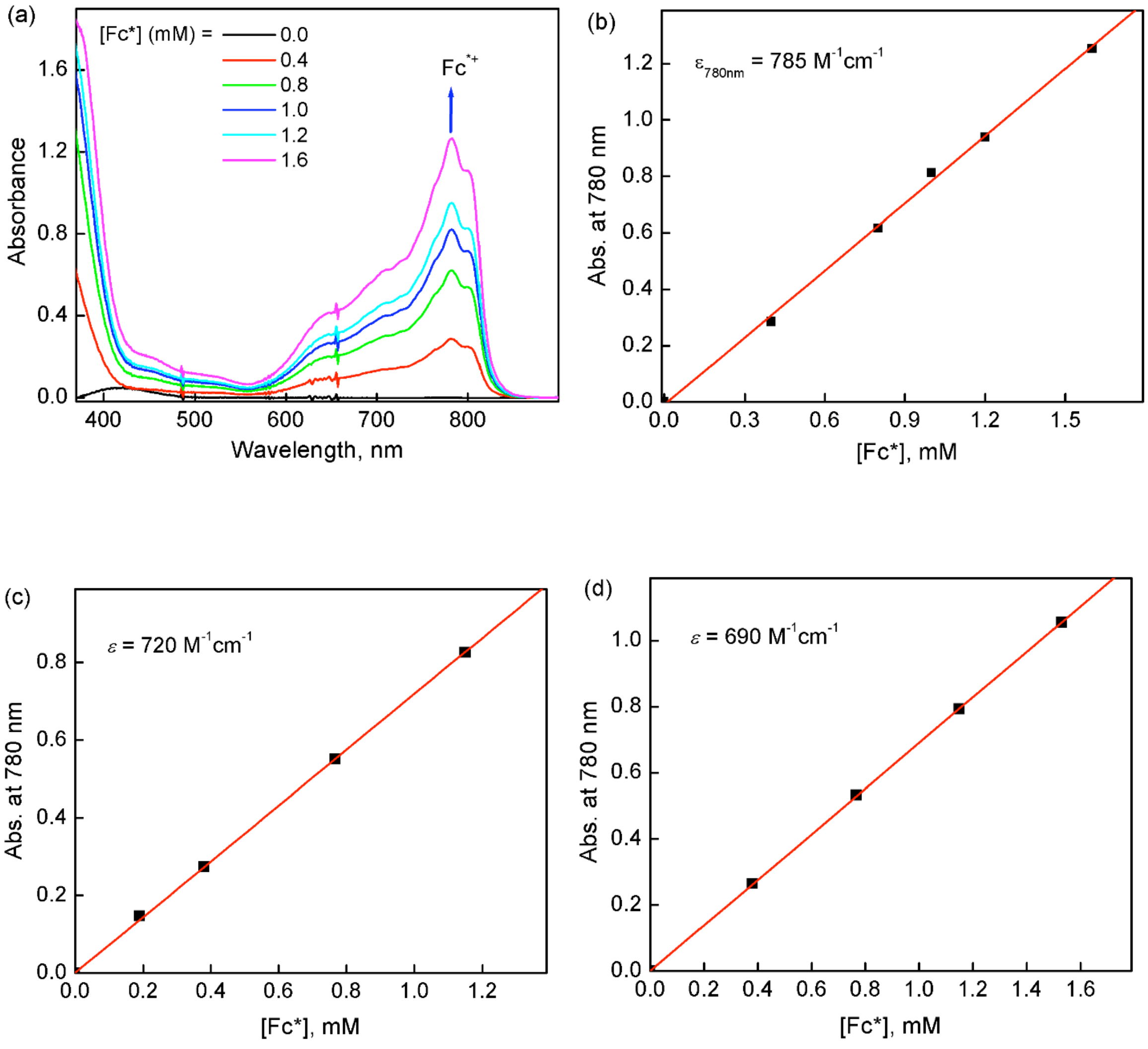

Figure S1. (a) Spectral titration for the formation of Fc^{*+} upon addition of Fc^{*} into the solution of excess amount of *p*-benzoquinone in the presence of HOTF (5.0 mM) in acetone at 193 K. (b, c, d) Plots of the absorbance at 780 nm due to Fc^{*+} generated from the reaction of Fc^{*} and excess amount of *p*-benzoquinone in the presence of HOTF (5.0 mM) vs. the concentration of Fc^{*} (b) (0.0 – 1.60 mM) at 193 K, (c) (0.0 – 1.15 mM) at 213 K and (d) (0.0 – 1.15 mM) at 223 K to determine the extinction coefficient of Fc^{*+} in acetone.

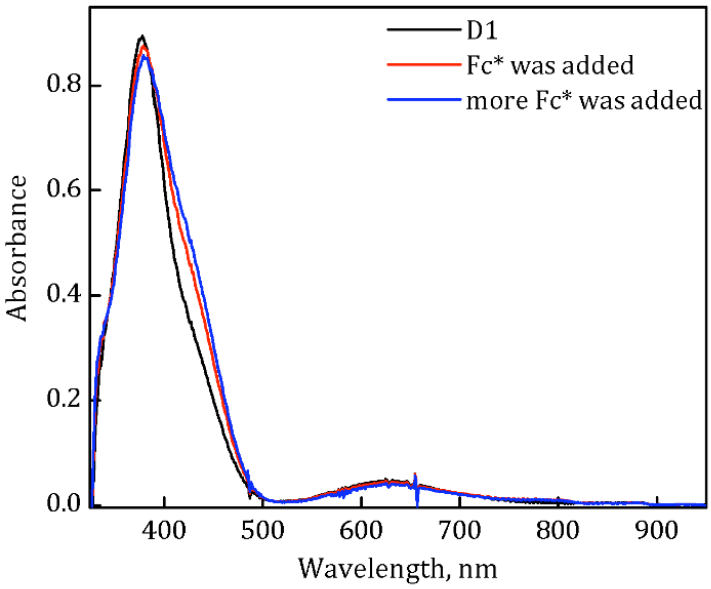

Figure S2. UV-visible spectra of **D1** (0.20 mM) (black line) and **D1** (0.20 mM) plus Fc* (red line (1.0 mM) and blue line (2.0 mM)) in acetone at 223 K.

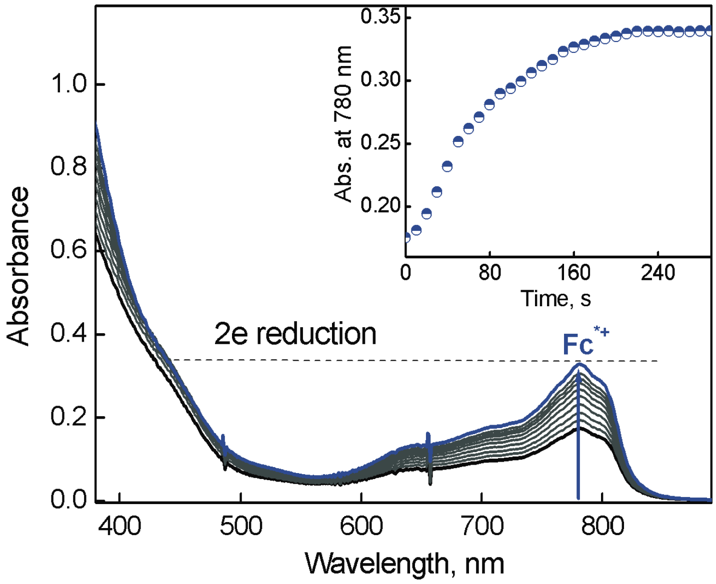

Figure S3. UV-vis spectral changes observed in the two-electron reduction of O_2 (0.22 mM) catalyzed by **D1** (0.10 mM) with Fc^* (2.0 mM) in the presence of HOTF (4.0 mM) in acetone at 223 K. Inset shows the time profile of the absorbance at 780 nm due to Fc^{*+}.

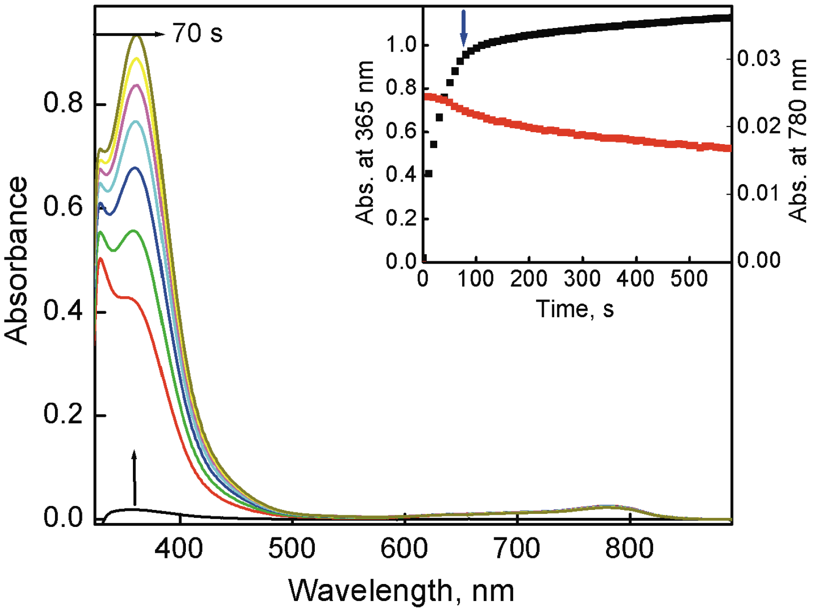

Figure S4. UV-vis spectral changes observed in the reaction of NaI (0.20 M) with the diluted (×15) acetone solution of the products at 298 K after the complete catalytic reduction of O_2 (11.0 mM) by **D1** (0.10 mM) with Fc^* (0.80 mM) in the presence of HOTF (2.0 mM) in acetone at 213 K.

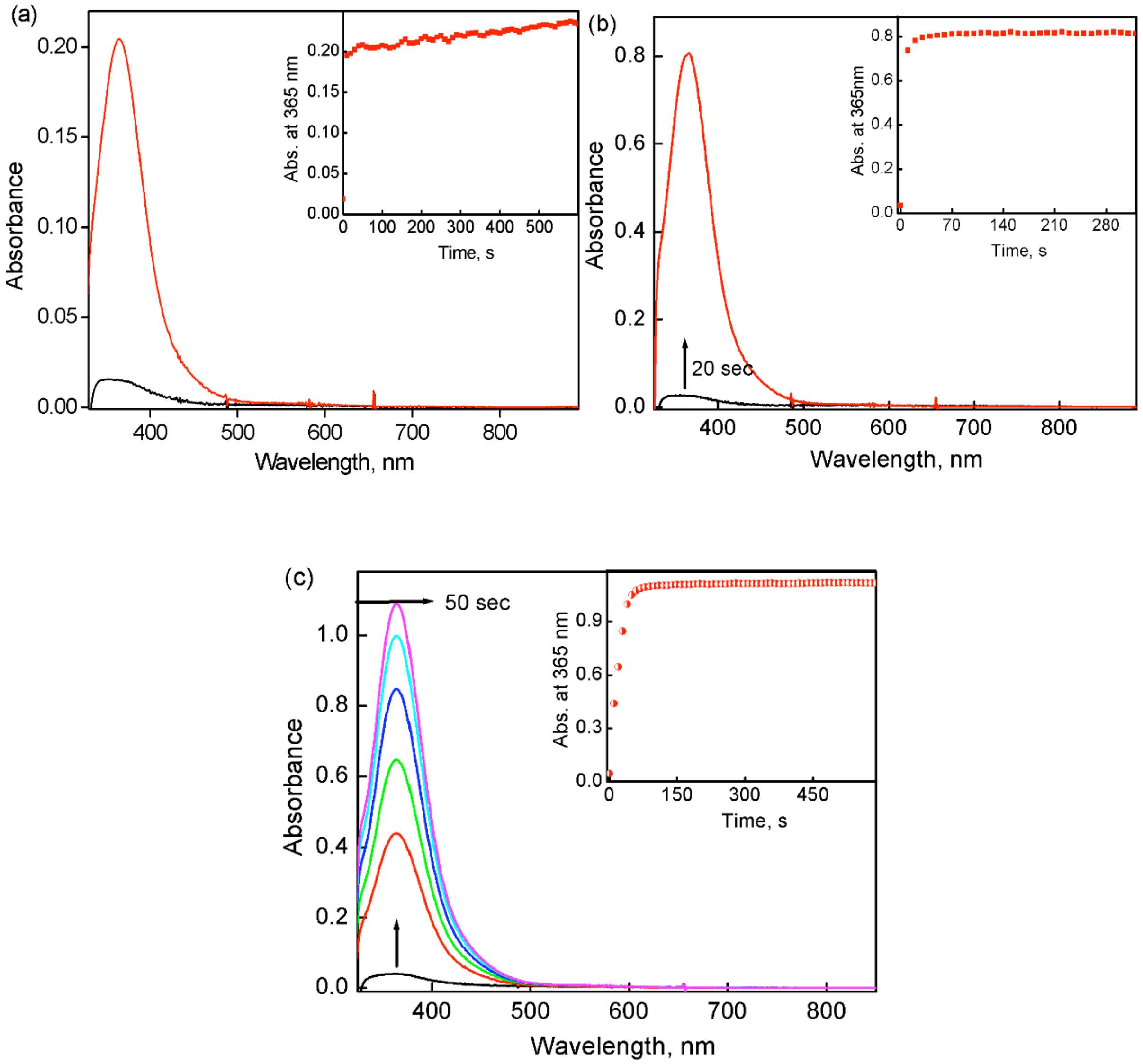

Figure S5. UV-visible spectral changes observed in the formation reaction of I_3^- upon addition of (a) an acetone solution containing **D1** (7.0 µM) and HOTF (70 µM) into NaI (0.20 M) in acetone at 298 K, (b) an acetone solution containing H_2O_2 (33.0 µM) into NaI (0.20 M) in acetone at 298 K and (c) an acetone solution containing H_2O_2 (33.0 µM), **D1** (7.0 µM) and HOTF (70 µM) mixed for 1.5 h into NaI (0.20 M) in acetone at 298 K.

Note: Comparing the absorbance of I_3^- at 365 nm in part c with that in part a and b clearly shows that exactly the same amount of I_3^- in the presence of **D1** (c) is produced as in the absence of **D1** in the reaction of H_2O_2 and I^- (b). Moreover according to the time course of the formation of I_3^- the reaction of H_2O_2 and I^- is decelerated by the presence of **D1** (part c).

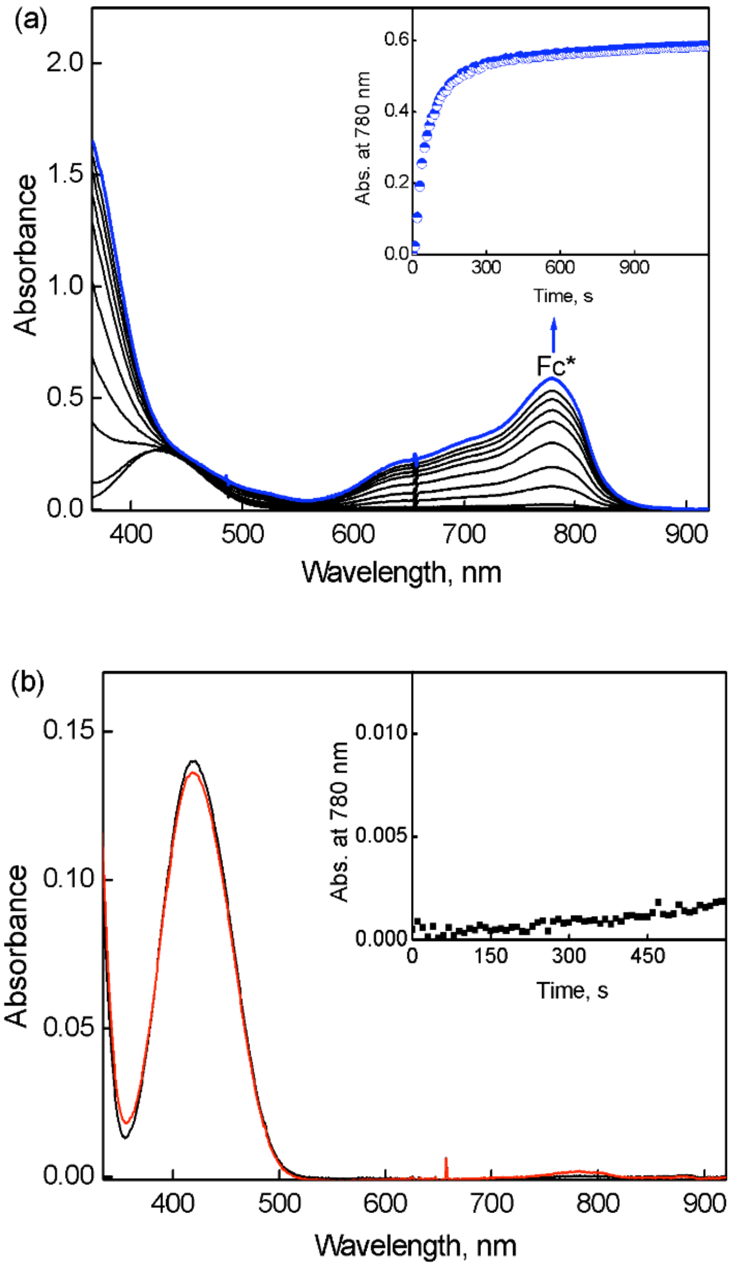

Figure S6. UV-vis spectral changes observed in the reaction of Fc^* (2.0 mM at 298 K (a) and 1.0 mM at 223 K (b) and H_2O_2 (0.40 mM) in the presence of HOTF (4.0 mM) in acetone. Inset shows the time profile of the absorbance at 780 nm due to Fc^{*+}.

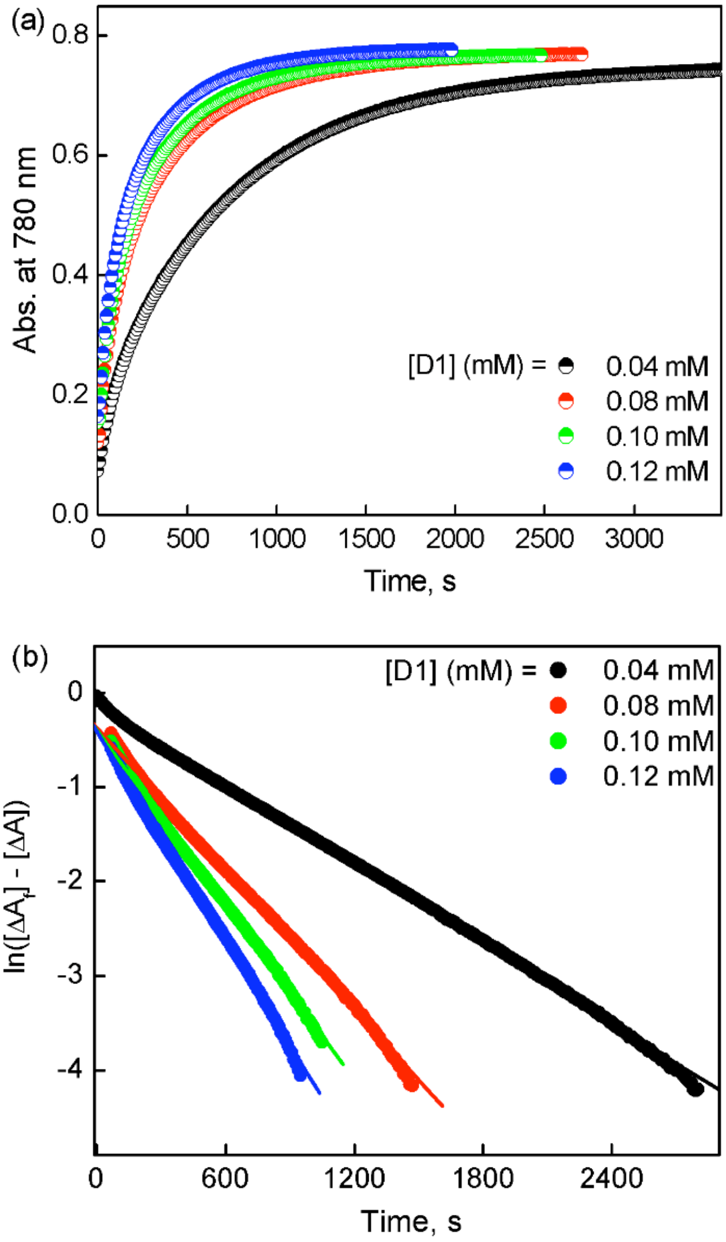

Figure S7. (a) Time profiles of the absorbance at 780 nm due to Fc^{*+} and (b) first-order plots of the formation of Fc^{*+} in the two-electron reduction of O_2 catalyzed by **D1** (0.040 – 0.12 mM) with Fc^* (1.0 mM) in the presence of HOTF (3.0 mM) in O_2-saturated acetone ($[O_2]$ = 11.0 mM) at 223 K.

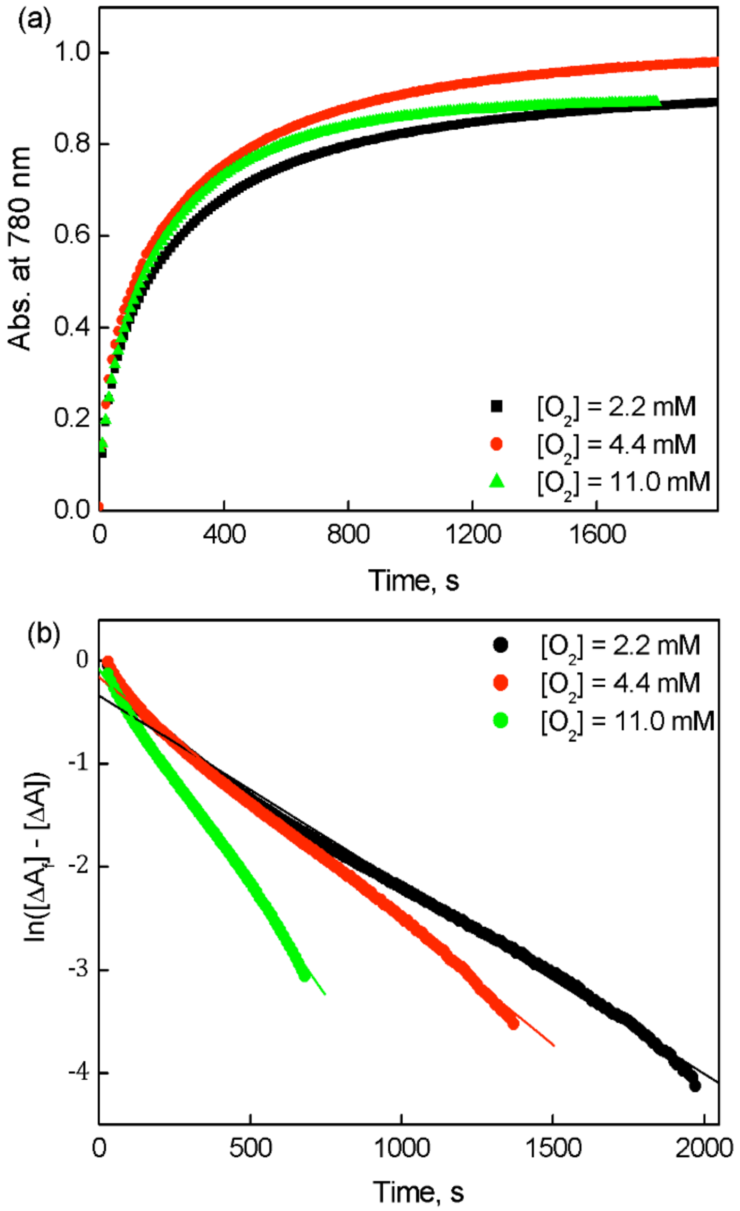

Figure S8. (a) Time profiles of the absorbance at 780 nm due to Fc^{*+} and (b) first-order plots of the formation of Fc^{*+} in the two-electron reduction of O_2 (2.2 – 11.0 mM) catalyzed by **D1** (0.10 mM) with Fc* (1.4 mM) in the presence of HOTF (3.0 mM) in acetone at 223 K.

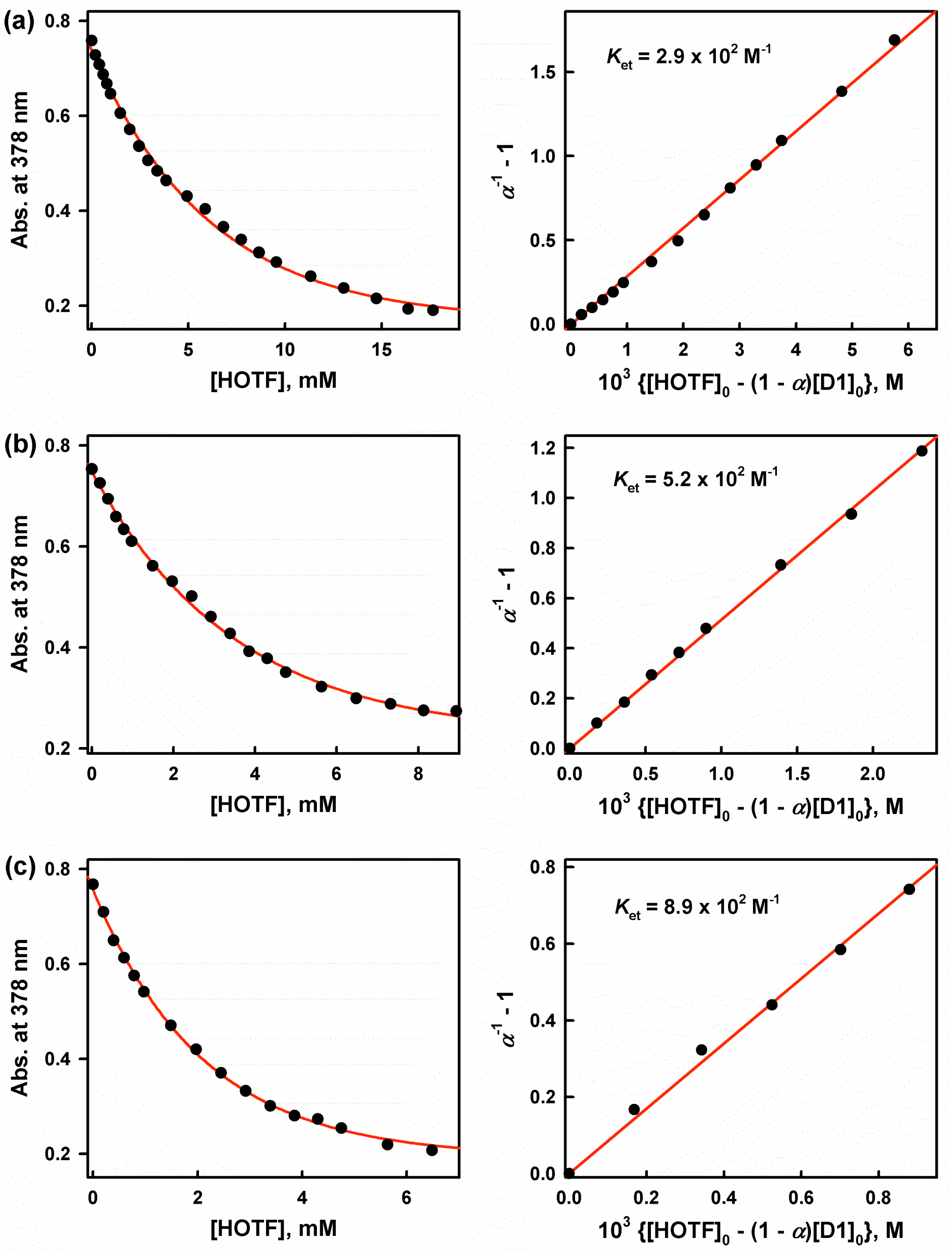

Figure S9. Absorbance changes of **D1** monitored at 378 nm upon addition of HOTF into the solution of **D1** (0.20 mM) in acetone at 273 K (a), 253 K (b) and 233 K (c) (left panels). Right panels show the plots of $\alpha^{-1} - 1$ vs $\{[\mathrm{HOTF}]_0 - (1 - \alpha)[\mathbf{D1}]_0\}$ to determine the equilibrium constants (K_{eq}) in the protonation of **D1** in acetone, respectively.

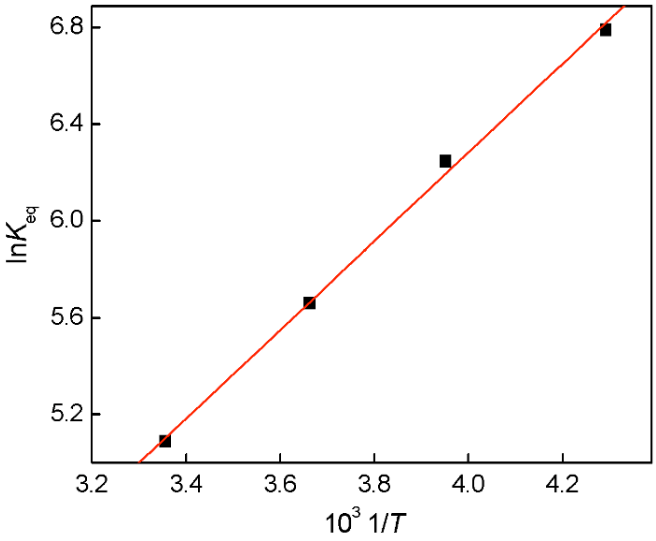

Figure S10. Van't Hoff plot to determine the enthalpy and entropy changes in the protonation of **D1** upon addition of HOTF (0.0 – 28.0 mM) into the solution of **D1** (0.20 mM) in acetone at 298K.

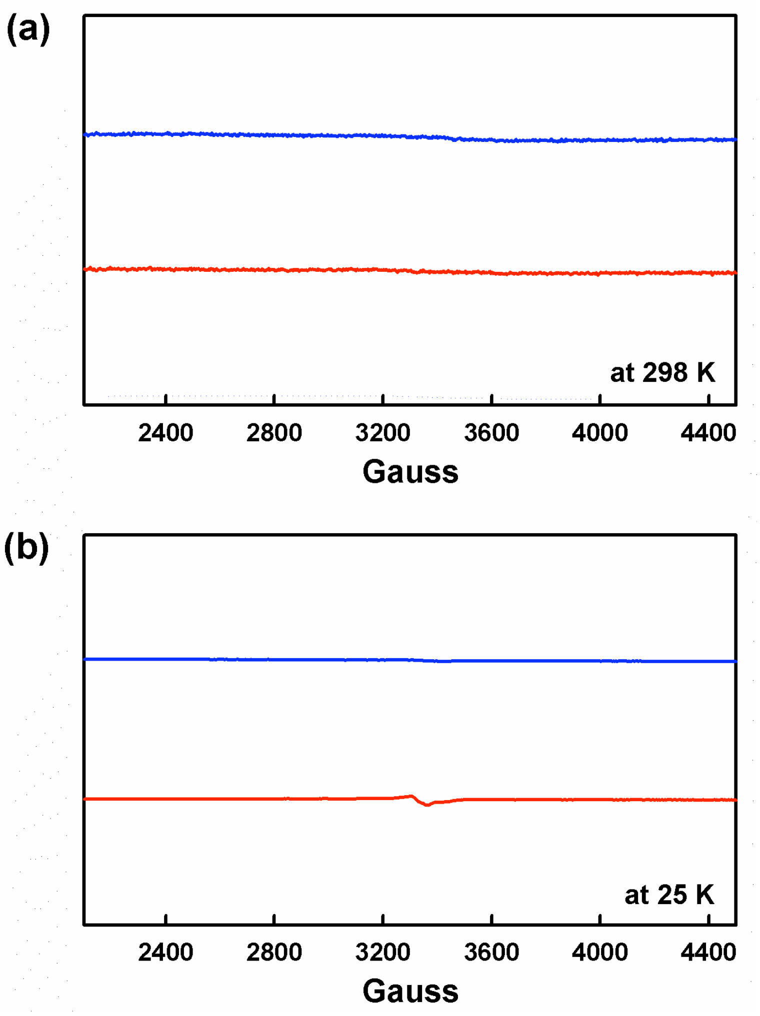

Figure S11. (a) X-band EPR spectra of **D1** (8.0 mM) in the absence (blue line) and presence (red line) of HOTF (40 mM) at 298 K in acetone. (b) X-band EPR spectra of **D1** (1.0 mM) in the absence (blue line) and presence (red line) of HOTF (5.0 mM) at 25 K in acetone.

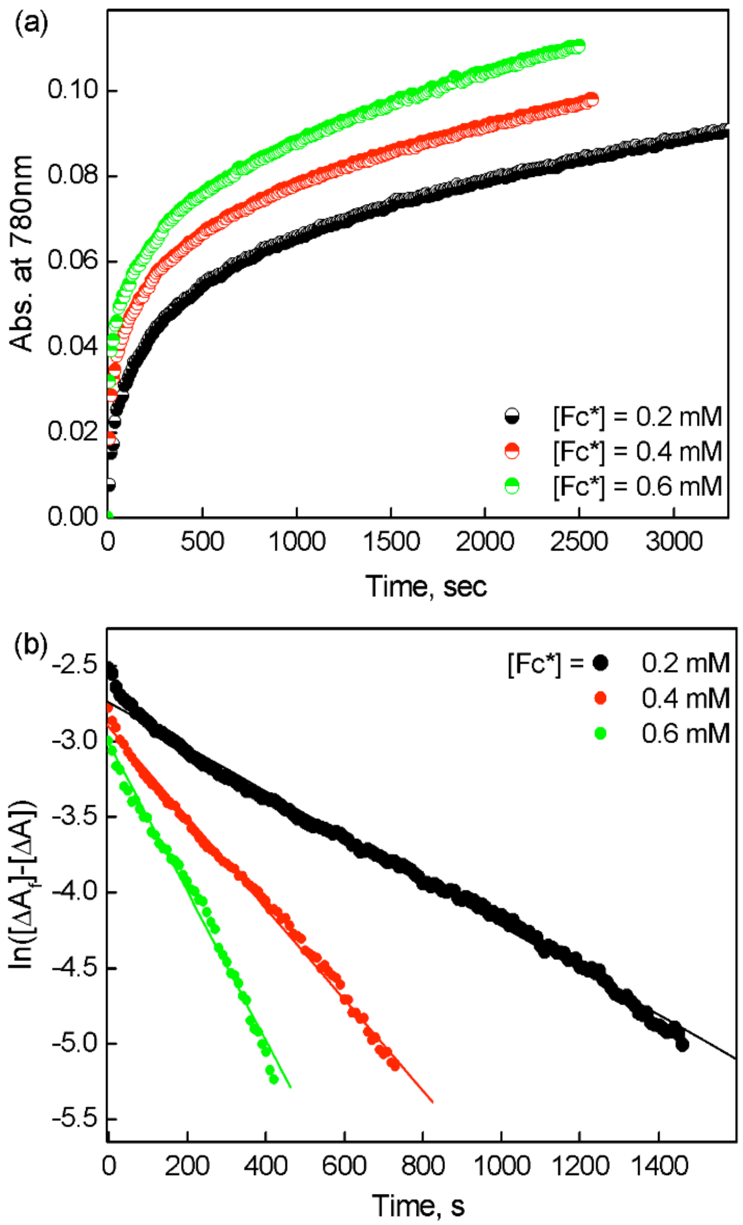

Figure S12. (a) Time profiles of the absorbance at 780 nm due to Fc^{*+} and (b) first-order plots of first electron transfer from Fc^{*} (0.20 mM (black), 0.40 mM (red) and 0.60 mM (green)) to **D1** (0.10 mM) in the presence of HOTF (3.0 mM) in acetone at 203 K.

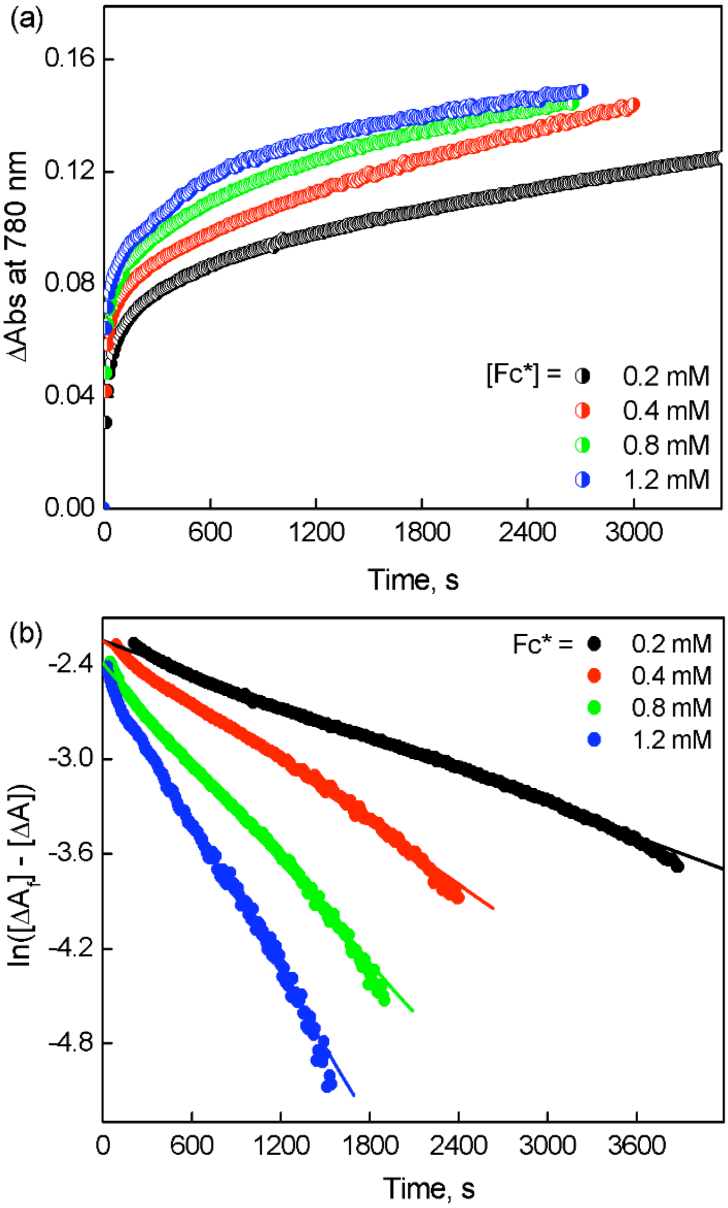

Figure S13. (a) Time profiles of the absorbance at 780 nm due to Fc^{*+} and (b) first-order plots of second electron transfer from Fc^{*} (0.20 mM (black), 0.40 mM (red), 0.80 mM (green) and 1.2 mM (blue)) to **D1** (0.10 mM) in the presence of HOTF (3.0 mM) in acetone at 213 K.

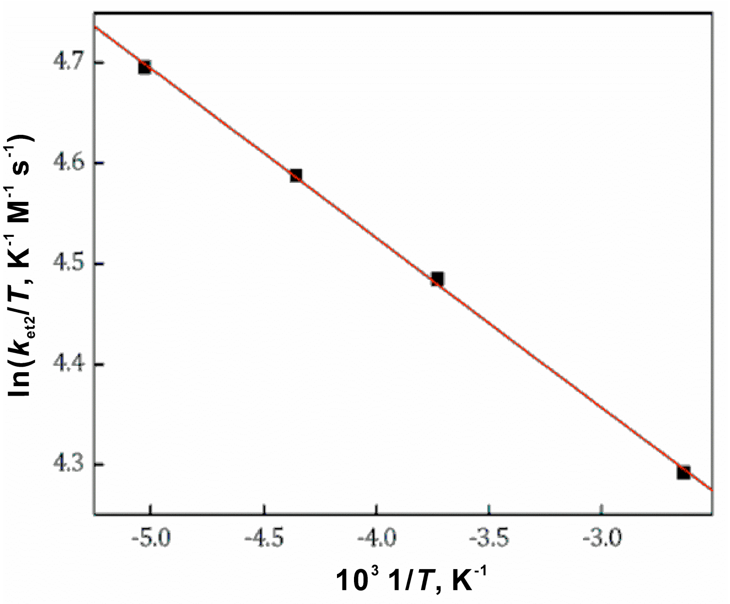

Figure S14. Eyring plot, $\ln(k_{et2}/T)$ vs $1/T$, of the rate constants (k_{et2}) of electron transfer from Fc^* to **D2** in acetone.